Calculation of the gating charge for the Kv1.2 voltage–activated potassium channel

Fatemeh Khalili-Araghi, Vishwanath Jogini, Vladimir Yarov–Yarovoy, Emad Tajkhorshid, Benoît Roux, and Klaus Schulten

Supplementary Information

Construction of the Atomic Models

The simulation systems of the full channel represent atomic models of the Kv1.2 channel embedded into a DPPC lipid bilayer surrounded by an aqueous salt solution of 500 mM KCl. The initial coordinates of the Kv1.2 channel in the active and the resting state were assembled from the atomic models of Pathak et al [1]. The procedure of constructing the protein/membrane system is described in [2]. The symmetry axis of the channel is aligned along the membrane normal (z-axis) with the center of the bilayer at $z = 0$. All histidine residues were assigned HSP protonation states carrying a net charge of +1. All other titratable residues were modeled in their default ionization state. The pKa calculation provided in the Supplementary Material shows that the protonation states chosen are consistent with most representative ionization state of the charged residues. To achieve a salt concentration of 500 mM, 307 K^+ ions and 279 Cl^- ions were added to the bulk solution. In addition, two K^+ ions were positioned at two of the previously identified binding sites in the selectivity filter, with a third K^+ ion in the central cavity. The resulting systems are electrically neutral and each comprise $\sim$ 350,000 atoms.

The active state, was equilibrated for 3 ns with the protein backbone restrained harmonically, and was then equilibrated further for 97 ns without restraints. A constant electric field (in the z-direction), corresponding to a voltage bias of +500 mV across the membrane, was applied to stablize the system in the open conformation. The resting state, was equilibrated following a multistage protocol. The system was simulated for 3 ns with the protein backbone restrained. For the next 50 ns of equilibration the backbone dihedral angles (ϕ and ψ) of residues 293-306 on S4, 311-323 of the S4-S5 linker, and 390-411 of S6 were constrained harmonically with a force constant of 5 (kcal/mol)·rad^{-2}. In addition, a flat bottom harmonic constraint with minimum distances of 4.0, 1.8, and 1.8 Å and a force constant of 1 (kcal/mol)·Å^{-2} was imposed between the CZ, H22, and HE atoms of R294 (on S4), and the CD, OE1, and OE2 atoms of E226 (on S2) in all four subunits. The C_α atoms of residues 410 and 411 (on S6) in diagonal subunits were also constrained to a maximum distance of 11.5 Å with a force constant of 5 (kcal/mol)·Å^{-2}. The dihedral restraints on S4 and distance restraints between R294 and E226 were released after 50 ns, and the system was simulated for another 50 ns. A constant electric field (in the z-direction) corresponding to a voltage bias of -500 mV across the membrane was applied to stabilize the system in the closed conformation. The equilibration simulations were performed at the temperature of 333 K.

The voltage-sensor domains (VSD) of Kv1.2 in the active and resting states were also placed individually

into DPPC bilayers, surrounded by 100 mM KCl solution. The simulated systems (shown in Fig. S1) included the S1-S4 segments and the S4-S5 linker of Kv1.2 (residues 161–324). The protein was inserted into a pre-equilibrated and hydrated DPPC lipid bilayer, using the program VMD (3). An aqueous solution with 38 K^+ and 41 Cl^- ions was added on both sides of the DPPC patch to neutralize the simulated system and ensure physiological salt concentrations. The total number of atoms in the VSD/membrane systems were $\sim$ 94,000.

Following 5000 steps of energy minimization with all protein atoms constrained, the VSD systems were equilibrated for 1.5 ns with the protein backbone restrained. The active and resting states were equilibrated then with applied electric fields, corresponding to +250 mV and -250 mV transmembrane potentials, for the active and the resting state, respectively. The active state proved to be stable after 50 ns of equilibration; the resting state needed to be simulated for another 50 ns to achieve a root mean square fluctuation (RMSF) below 3 Å for the protein backbone in the transmembrane region, indicating stability. The RMSF of the VSD is plotted in Fig. S3B. During all the simulations, the backbone atoms of residues 312–324 (S4-S5 linker) were restrained harmonically, with a force constant of 1 (kcal/mol)·Å^{-2}. The VSD simulations were carried out at the temperature of 318 K. The simulations performed are summarized in Table 3 of the Supplementary Material.

The configuration of the VSD resulting from the 50 ns and 100 ns equilibration runs, were used to simulate the active and resting states subject to three different voltage biases. Each protein state was simulated at -250 mV, 0 mV, and +250 mV and each simulation lasted for 50 ns. The equilibrated configurations of the full tetrameric channel, resulting from 100 ns of equilibration runs were also simulated at two different voltage biases. The active and resting states were each simulated for 50 ns, at a positive voltage of +500 mV and a negative voltage of -500 mV. A summary of all the simulations is provided in Table 3. Despite the large magnitude of the voltage applied (compared to physiological values of $\sim$100 mV), the average root mean square deviation (RMSD) of the protein backbone from the equilibrated conformations were < 7 Å (shown in Table 6 of the Supplementary Material) in all ten simulations, allowing us to calculate the total gating charge for the full tetrameric channel, as well as for the individual VSD, from the average displacement charge Q_d.

Free Energy Perturbation

All-atom FEP/MD simulations were carried out for the isolated VSD and the tetrameric channel. The FEP/MD calculations are probing the membrane potential felt by key charged residues of the voltage-

sensor domains that are within the transmembrane region. The charging free energy of each amino acid side chain was calculated at multiple membrane voltage. The difference between the two free energies thus obtained represents the energetic coupling of the charged residue to the transmembrane potential, and corresponds to the fraction of the transmembrane field acting on q_i when the protein is in the open or closed state.

Starting configurations of the VSD for each state were taken from 100 ns equilibration simulations (SimVSD1-p, and SimVSD2-eq). Prior to the FEP/MD calculations, each state was equilibrated for an additional 10 ns with three different membrane voltages (±1 V and 0 V). Separate FEP/MD trajectories were generated (for each residue) with the thermodynamic coupling parameter λ varying between 0 and 1, in increments of 0.25. The calculation for each value of λ included 50 ps of initial equilibration and 150 ps of data collection, from which the free energies were calculated using the weighted histogram analysis method (WHAM) (4).

Five starting configurations for the full tetrameric channel were selected at every 8 ns from the 50 ns trajectories. The charging free energies were then calculated for the charged residues of each protein state, at +500 mV and -500 mV voltages. Nine separate FEP/MD trajectories were generated for each residue (perturbed simultaneously in all four subunits), with λ varying betwen 0 and 1, in increments of 0.125. The calculations for each λ included 50 ps of initial equilibration and 200 ps of data collection. The free energies were then obtained using WHAM (4). The statistical uncertainty on the results is estimated from the standard deviation for the five separate FEP/MD calculations.

Electrostatic Potential Maps

Electrostatic potential maps were calculated using the PME plugin (5) of the program VMD (3). The maps were calculated for the active state trajectories of the full channel at +500mV and -500 mV (SimOpen-p and SimOpen-n), and the closed state trajectories at +500 mV and -500 mV (SimClosed-p and SimClosed-n). The time-averaged maps are then used to extract the transmembrane potential along the center of the VSD, in each protein state. In the case of the isolated VSD, the electrostatic maps were obtained for the active state trajectories at 1 V and 0 V (SimVSD1-1V and SimVSD1-0V), and the resting state trajectories at -1 V and 0 V(SimVSD2-1V and SimVSD2-0V). For each protein state, the transmembrane potential is then plotted along a straight line parallel to the $z-$axis passing through the VSD.

Steered molecular dynamics simulations

Steered molecular dynamics (SMD) simulations (6; 7) were carried out on the final conformation of the closed states obtained from equilibration simulations of the individual VSD and the tetrameric channel. During SMD simulations the coordinates of CZ atoms of R1 were pulled down toward the intracellular solution using a harmonic constraint moving with a constant velocity of 0.5 Å/ns, and a force constant of 5 (kcal/mol).Å^{-2}. The simulations lasted 30–35 ns. In the case of the tetrameric channel, all four residues (R1) in the tetrameric channel were pulled with the forces being applied to the center of mass of the four arginine side chain carbon atoms. The pore domain (residues 325–421) was restrained harmonically, in order to prevent net translation of the protein. The isolated VSD simulations were performed with the S4-S4 linker (residues 312–325) constrained, as in the case of the equilibration simulations.

pKa calculations

The changes in pKa were calculated from a continuum electrostic approximation according as the free energy difference between the unprotonated and protonated residue in the full system relative to the fragment alone (8). The free energy differences were calculated from an equilibrated conformation of the Kv1.2 channel in the open and the closed state taken from the MD simulations. The continuum electrostatic calculations used to determine the protonation states of ionizable residues in the VSD were carried out using the finite-difference Poisson-Boltzmann solver PBEQ (9) of the program CHARMM (10). For each residue, the calculations were first carried out using a coarse grid of 1.2 Å spacing, followed by a focussing step using a fine grid spacing of 0.5 Å. A cubic grid of 180^3 points was used. The membrane, of thickness 25 Å was represented explicitly from the hydrocarbon chains of the lipids included in the MD simulations. The dielectric constant of the aqueous region was set to 80, the dielectric constant of the protein region was set to 4, and the the dielectric constant of the membrane region was set to 2. The set of atomic radii optimized from free energy simulations was used to set the dielectric boundary (11). The calculations are limited to the Arg, Lys, Asp, Glu and His residues of the VSD, which is the main interest for the present study, for a total of 40 pKa calculations, The average charged state were calculated by assuming a pH of 7. The results are reported in Table 1 and Table 2.

The calculation shows that all the Glu and Asp have a charge of -1, which corresponds to their default ionization state. Similarly, most of the Arg have a charge of +1, with the exception of Arg303 for 1-2 subunits. All the Lys have a charge of +1, with the exception of Lys306 in the closed state for a

few subunits. The His display more complicated behaviors, although only His310 is really partially in the functional region of the VSD. However, the His do not participate to the gating charge, as they are not coupled to the transmembrane potential. It is important to note that the gating charges are not titrable (12). Furthermore, the calculated charged state are extremely sensitive to the approximations made, and it is important to consider those results as suggestive at best.

It can be conclude that the default charged state assumed for the main ionizable residues of the VSD is valid. Those include: R294 (R1), R297 (R2), R300 (R3), R303 (R4), K306 (K5), R309 (R6) along S4, E183 (E0) along S1, E226 (E1) and E236 (E2) along S2, and D259 (D3) along S3.

Supplementary Table 1: Results for the closed state

Residue	$\Delta\Delta G$	ΔpKa	Q_{MD}	$\langle Q \rangle_{\mathrm{pKa}}$
ASP 190	-0.104	0.076	-1.000	-0.999
ASP 190	-0.792	0.577	-1.000	-0.997
ASP 190	-0.464	0.338	-1.000	-0.998
ASP 190	-0.368	0.268	-1.000	-0.999
ASP 194	-0.282	0.205	-1.000	-0.999
ASP 194	1.015	-0.739	-1.000	-1.000
ASP 194	2.071	-1.509	-1.000	-1.000
ASP 194	3.523	-2.566	-1.000	-1.000
ASP 220	0.438	-0.319	-1.000	-1.000
ASP 220	0.443	-0.322	-1.000	-1.000
ASP 220	2.223	-1.619	-1.000	-1.000
ASP 220	1.003	-0.730	-1.000	-1.000
ASP 259	10.803	-7.870	-1.000	-1.000
ASP 259	11.915	-8.680	-1.000	-1.000
ASP 259	7.578	-5.521	-1.000	-1.000
ASP 259	7.217	-5.258	-1.000	-1.000
ASP 280	-0.106	0.077	-1.000	-0.999
ASP 280	0.692	-0.504	-1.000	-1.000
ASP 280	-0.343	0.250	-1.000	-0.999
ASP 280	-0.482	0.351	-1.000	-0.998

GLU 154	1.142	-0.832	-1.000	-1.000
GLU 154	0.343	-0.250	-1.000	-0.999
GLU 154	0.469	-0.342	-1.000	-0.999
GLU 154	-0.390	0.284	-1.000	-0.998
GLU 157	0.020	-0.015	-1.000	-0.999
GLU 157	1.459	-1.063	-1.000	-1.000
GLU 157	0.359	-0.262	-1.000	-0.999
GLU 157	-1.076	0.784	-1.000	-0.993
GLU 183	0.446	-0.325	-1.000	-0.999
GLU 183	0.904	-0.658	-1.000	-1.000
GLU 183	1.256	-0.915	-1.000	-1.000
GLU 183	0.308	-0.224	-1.000	-0.999
GLU 191	0.593	-0.432	-1.000	-1.000
GLU 191	0.344	-0.251	-1.000	-0.999
GLU 191	1.631	-1.188	-1.000	-1.000
GLU 191	-0.301	0.219	-1.000	-0.998
GLU 193	2.718	-1.980	-1.000	-1.000
GLU 193	4.425	-3.223	-1.000	-1.000
GLU 193	-0.673	0.490	-1.000	-0.996
GLU 193	2.799	-2.039	-1.000	-1.000
GLU 226	0.620	-0.452	-1.000	-1.000
GLU 226	4.284	-3.121	-1.000	-1.000
GLU 226	0.115	-0.084	-1.000	-0.999
GLU 226	0.769	-0.560	-1.000	-1.000
GLU 236	9.358	-6.817	-1.000	-1.000
GLU 236	8.675	-6.320	-1.000	-1.000
GLU 236	9.432	-6.871	-1.000	-1.000
GLU 236	3.674	-2.676	-1.000	-1.000
GLU 273	1.435	-1.045	-1.000	-1.000
GLU 273	0.734	-0.535	-1.000	-1.000
GLU 273	2.094	-1.526	-1.000	-1.000
GLU 273	-0.891	0.649	-1.000	-0.995

GLU 276	-0.481	0.351	-1.000	-0.997
GLU 276	-0.459	0.334	-1.000	-0.997
GLU 276	-0.495	0.360	-1.000	-0.997
GLU 276	-0.323	0.235	-1.000	-0.998
GLU 279	-0.577	0.420	-1.000	-0.997
GLU 279	0.134	-0.098	-1.000	-0.999
GLU 279	-0.932	0.679	-1.000	-0.994
GLU 279	-0.727	0.529	-1.000	-0.996
ARG 163	1.407	-1.025	1.000	1.000
ARG 163	-2.153	1.569	1.000	1.000
ARG 163	-0.438	0.319	1.000	1.000
ARG 163	0.468	-0.341	1.000	1.000
ARG 189	-3.278	2.388	1.000	1.000
ARG 189	-3.152	2.296	1.000	1.000
ARG 189	-0.175	0.127	1.000	1.000
ARG 189	-5.512	4.015	1.000	1.000
ARG 240	2.852	-2.078	1.000	1.000
ARG 240	-1.822	1.327	1.000	1.000
ARG 240	2.421	-1.764	1.000	1.000
ARG 240	-2.439	1.777	1.000	1.000
ARG 294	-4.547	3.312	1.000	1.000
ARG 294	-5.888	4.289	1.000	1.000
ARG 294	-4.484	3.267	1.000	1.000
ARG 294	-6.315	4.600	1.000	1.000
ARG 297	-0.044	0.032	1.000	1.000
ARG 297	3.889	-2.833	1.000	0.998
ARG 297	1.816	-1.323	1.000	1.000
ARG 297	-1.988	1.448	1.000	1.000
ARG 300	2.958	-2.155	1.000	1.000
ARG 300	4.484	-3.267	1.000	0.994
ARG 300	3.644	-2.655	1.000	0.999
ARG 300	2.809	-2.046	1.000	1.000

ARG 303	7.983	-5.816	1.000	0.316
ARG 303	5.243	-3.819	1.000	0.979
ARG 303	7.020	-5.114	1.000	0.699
ARG 303	1.747	-1.273	1.000	1.000
ARG 309	2.292	-1.670	1.000	1.000
ARG 309	2.441	-1.778	1.000	1.000
ARG 309	-0.959	0.699	1.000	1.000
ARG 309	1.989	-1.449	1.000	1.000
LYS 247	0.421	-0.307	1.000	0.999
LYS 247	-3.803	2.770	1.000	1.000
LYS 247	-2.422	1.764	1.000	1.000
LYS 247	0.594	-0.433	1.000	0.999
LYS 277	-5.057	3.684	1.000	1.000
LYS 277	-6.828	4.974	1.000	1.000
LYS 277	-4.694	3.419	1.000	1.000
LYS 277	-1.721	1.254	1.000	1.000
LYS 306	5.118	-3.728	1.000	0.393
LYS 306	6.046	-4.404	1.000	0.120
LYS 306	7.097	-5.170	1.000	0.023
LYS 306	3.105	-2.262	1.000	0.950
LYS 312	-1.061	0.773	1.000	1.000
LYS 312	-4.474	3.259	1.000	1.000
LYS 312	-6.355	4.630	1.000	1.000
LYS 312	-4.949	3.605	1.000	1.000
HSP1 196	-1.480	1.078	1.000	0.567
HSP2 196	-7.282	5.305	1.000	1.000
HSP1 196	-0.955	0.696	1.000	0.352
HSP2 196	-2.321	1.691	1.000	0.843
HSP1 196	-0.359	0.262	1.000	0.167
HSP2 196	-0.384	0.279	1.000	0.173
HSP1 196	-0.623	0.454	1.000	0.238
HSP2 196	-1.830	1.333	1.000	0.703

HSP1 203	-0.329	0.239	1.000	0.160
HSP2 203	-1.043	0.760	1.000	0.387
HSP1 203	-6.657	4.849	1.000	1.000
HSP2 203	-8.639	6.293	1.000	1.000
HSP1 203	-1.081	0.787	1.000	0.402
HSP2 203	-0.998	0.727	1.000	0.369
HSP1 203	-1.291	0.940	1.000	0.489
HSP2 203	-6.748	4.916	1.000	1.000
HSP1 310	2.838	-2.067	1.000	0.001
HSP2 310	3.533	-2.574	1.000	0.000
HSP1 310	1.725	-1.257	1.000	0.006
HSP2 310	1.754	-1.278	1.000	0.006
HSP1 310	0.293	-0.213	1.000	0.063
HSP2 310	-0.069	0.050	1.000	0.110
HSP1 310	-9.874	7.193	1.000	1.000
HSP2 310	-0.712	0.519	1.000	0.266

Supplementary Table 2: Results for the open state

Residue	$\Delta\Delta G$	ΔpKa	Q_{MD}	$\langle Q \rangle_{\mathrm{pKa}}$
ASP 190	0.361	-0.263	-1.000	-1.000
ASP 190	-1.530	1.114	-1.000	-0.990
ASP 190	0.978	-0.712	-1.000	-1.000
ASP 190	-0.291	0.212	-1.000	-0.999
ASP 194	1.514	-1.103	-1.000	-1.000
ASP 194	-0.291	0.212	-1.000	-0.999
ASP 194	-0.710	0.517	-1.000	-0.997
ASP 194	-1.286	0.937	-1.000	-0.993
ASP 220	-0.384	0.280	-1.000	-0.998
ASP 220	0.349	-0.254	-1.000	-1.000
ASP 220	-0.248	0.181	-1.000	-0.999
ASP 220	-0.422	0.307	-1.000	-0.998
ASP 259	5.861	-4.270	-1.000	-1.000
ASP 259	14.045	-10.232	-1.000	-1.000
ASP 259	10.495	-7.646	-1.000	-1.000
ASP 259	15.719	-11.451	-1.000	-1.000
ASP 280	-1.175	0.856	-1.000	-0.994
ASP 280	-0.187	0.136	-1.000	-0.999
ASP 280	-0.002	0.001	-1.000	-0.999
ASP 280	-1.030	0.750	-1.000	-0.996
GLU 154	0.446	-0.325	-1.000	-0.999
GLU 154	0.850	-0.619	-1.000	-1.000
GLU 154	-0.223	0.162	-1.000	-0.998
GLU 154	-0.332	0.242	-1.000	-0.998
GLU 157	0.222	-0.162	-1.000	-0.999
GLU 157	-0.308	0.224	-1.000	-0.998
GLU 157	0.106	-0.077	-1.000	-0.999
GLU 157	0.047	-0.034	-1.000	-0.999
GLU 183	3.288	-2.395	-1.000	-1.000

GLU 183	1.485	-1.082	-1.000	-1.000
GLU 183	2.448	-1.783	-1.000	-1.000
GLU 183	0.975	-0.710	-1.000	-1.000
GLU 191	4.340	-3.162	-1.000	-1.000
GLU 191	-1.215	0.885	-1.000	-0.991
GLU 191	-0.917	0.668	-1.000	-0.995
GLU 191	-0.742	0.540	-1.000	-0.996
GLU 193	1.668	-1.215	-1.000	-1.000
GLU 193	0.522	-0.381	-1.000	-1.000
GLU 193	1.547	-1.127	-1.000	-1.000
GLU 193	1.519	-1.106	-1.000	-1.000
GLU 226	5.116	-3.727	-1.000	-1.000
GLU 226	2.160	-1.574	-1.000	-1.000
GLU 226	3.977	-2.897	-1.000	-1.000
GLU 226	6.339	-4.618	-1.000	-1.000
GLU 236	6.379	-4.647	-1.000	-1.000
GLU 236	10.548	-7.684	-1.000	-1.000
GLU 236	8.346	-6.080	-1.000	-1.000
GLU 236	9.327	-6.795	-1.000	-1.000
GLU 273	-0.751	0.547	-1.000	-0.996
GLU 273	0.041	-0.030	-1.000	-0.999
GLU 273	-1.107	0.807	-1.000	-0.993
GLU 273	-1.118	0.814	-1.000	-0.992
GLU 276	-1.503	1.095	-1.000	-0.986
GLU 276	-1.167	0.850	-1.000	-0.992
GLU 276	-1.541	1.122	-1.000	-0.985
GLU 276	-0.934	0.680	-1.000	-0.994
GLU 279	-0.288	0.210	-1.000	-0.998
GLU 279	-0.148	0.108	-1.000	-0.998
GLU 279	2.788	-2.031	-1.000	-1.000
GLU 279	0.938	-0.683	-1.000	-1.000
ARG 163	1.028	-0.749	1.000	1.000

ARG 163	1.515	-1.104	1.000	1.000
ARG 163	0.771	-0.562	1.000	1.000
ARG 163	0.960	-0.699	1.000	1.000
ARG 189	-7.197	5.243	1.000	1.000
ARG 189	-3.480	2.535	1.000	1.000
ARG 189	-7.699	5.609	1.000	1.000
ARG 189	-7.597	5.534	1.000	1.000
ARG 240	0.303	-0.221	1.000	1.000
ARG 240	-1.192	0.868	1.000	1.000
ARG 240	0.749	-0.546	1.000	1.000
ARG 240	0.006	-0.004	1.000	1.000
ARG 294	-2.251	1.640	1.000	1.000
ARG 294	-0.873	0.636	1.000	1.000
ARG 294	-0.341	0.248	1.000	1.000
ARG 294	-2.954	2.152	1.000	1.000
ARG 297	-0.179	0.130	1.000	1.000
ARG 297	-2.941	2.142	1.000	1.000
ARG 297	-2.511	1.829	1.000	1.000
ARG 297	-0.380	0.277	1.000	1.000
ARG 300	-6.097	4.442	1.000	1.000
ARG 300	-3.095	2.255	1.000	1.000
ARG 300	-4.699	3.423	1.000	1.000
ARG 300	-5.194	3.784	1.000	1.000
ARG 303	-2.943	2.144	1.000	1.000
ARG 303	-3.623	2.639	1.000	1.000
ARG 303	-4.435	3.231	1.000	1.000
ARG 303	-2.365	1.723	1.000	1.000
ARG 309	-5.432	3.957	1.000	1.000
ARG 309	-3.125	2.277	1.000	1.000
ARG 309	0.943	-0.687	1.000	1.000
ARG 309	0.459	-0.334	1.000	1.000
LYS 247	0.229	-0.167	1.000	1.000

LYS 247	0.402	-0.293	1.000	0.999
LYS 247	-1.321	0.962	1.000	1.000
LYS 247	0.117	-0.085	1.000	1.000
LYS 277	-0.644	0.469	1.000	1.000
LYS 277	-1.346	0.980	1.000	1.000
LYS 277	-1.003	0.730	1.000	1.000
LYS 277	-0.852	0.621	1.000	1.000
LYS 306	-7.683	5.597	1.000	1.000
LYS 306	-2.395	1.745	1.000	1.000
LYS 306	-2.778	2.024	1.000	1.000
LYS 306	-4.074	2.968	1.000	1.000
LYS 312	-4.125	3.005	1.000	1.000
LYS 312	-2.540	1.850	1.000	1.000
LYS 312	0.215	-0.157	1.000	1.000
LYS 312	-4.278	3.116	1.000	1.000
HSP1 196	-7.156	5.213	1.000	1.000
HSP2 196	-6.945	5.060	1.000	1.000
HSP1 196	-0.093	0.068	1.000	0.114
HSP2 196	-0.228	0.166	1.000	0.138
HSP1 196	-0.372	0.271	1.000	0.170
HSP2 196	-0.333	0.243	1.000	0.161
HSP1 196	-0.543	0.396	1.000	0.214
HSP2 196	-0.608	0.443	1.000	0.233
HSP1 203	-7.561	5.508	1.000	1.000
HSP2 203	-7.928	5.775	1.000	1.000
HSP1 203	-0.818	0.596	1.000	0.302
HSP2 203	-1.101	0.802	1.000	0.410
HSP1 203	-0.801	0.583	1.000	0.296
HSP2 203	-1.400	1.020	1.000	0.534
HSP1 203	-1.119	0.815	1.000	0.417
HSP2 203	-1.389	1.012	1.000	0.530
HSP1 310	0.738	-0.538	1.000	0.031

13

HSP2 310	1.411	-1.028	1.000	0.010
HSP1 310	2.000	-1.457	1.000	0.004
HSP2 310	1.958	-1.426	1.000	0.004
HSP1 310	4.145	-3.020	1.000	0.000
HSP2 310	3.648	-2.658	1.000	0.000
HSP1 310	1.952	-1.422	1.000	0.004
HSP2 310	1.665	-1.213	1.000	0.007

References

[1] Pathak, M. M., V. Yarov-Yarovoy, G. Agrawal, B. Roux, P. Barth, S. Kohout, F. Tombola, and E. Y. Isacoff. 2007. Closing in on the resting state of the Shaker K$^+$ channel. *Neuron*. 56:124–140.

[2] Jogini, V. and B. Roux. 2007. Dynamics of the Kv1.2 voltage-gated K$^+$ channel in a membrane environment. *Biophys. J.* 93:3070–3082.

[3] Humphrey, W., A. Dalke, and K. Schulten. 1996. VMD – Visual Molecular Dynamics. *J. Mol. Graphics*. 14:33–38.

[4] Kumar, S., D. Bouzida, R. H. Swendsen, P. A. Kollman, and J. M. Rosenberg. 1992. The weighted histogram analysis method for free-energy calculations on biomolecules. I. The method. *J. Comp. Chem.* 13:1011–1021.

[5] Aksimentiev, A. and K. Schulten. 2005. Imaging alpha-hemolysin with molecular dynamics: Ionic conductance, osmotic permeability and the electrostatic potential map. *Biophys. J.* 88:3745–3761.

[6] Isralewitz, B., J. Baudry, J. Gullingsrud, D. Kosztin, and K. Schulten. 2001. Steered molecular dynamics investigations of protein function. *Journal of Molecular Graphics and Modeling*. 19:13–25. Also in *Protein Flexibility and Folding*, L. A. Kuhn and M. F. Thorpe, editors, *Biological Modeling Series* (Elsevier).

[7] Sotomayor, M. and K. Schulten. 2007. Single-molecule experiments in vitro and in silico. *Science*. 316:1144–1148.

[8] Roux, B., S. Bernèche, and W. Im. 2000. Ion channels, permeation and electrostatics: insight into the function of KcsA. *Biochemistry*. 39:13295–13306.

[9] Im, W., D. Beglov, and B. Roux. 1998. Continuum solvation model: Electrostatic forces from numerical solutions to the Poisson-Bolztmann equation. *Comp. Phys. Comm.* 111:59–75.

[10] Brooks, B. R., C. L. Brooks, III, A. D. Mackerell, Jr., L. Nilsson, R. J. Petrella, B. Roux, Y. Won, G. Archontis, C. Bartels, S. Boresch, A. Caflisch, L. Caves, Q. Cui, A. R. Dinner, M. Feig, S. Fischer, J. Gao, M. Hodoscek, W. Im, K. Kuczera, T. Lazaridis, J. Ma, V. Ovchinnikov, E. Paci, R. W. Pastor, C. B. Post, J. Z. Pu, M. Schaefer, B. Tidor, R. M. Venable, H. L. Woodcock, X. Wu, W. Yang, D. M. York, and M. Karplus. 2009. Charmm: The biomolecular simulation program. *J. Comp. Chem.* 30:1545–1614.

[11] Nina, M., D. Beglov, and B. Roux. 1997. Atomic Radii for Continuum Electrostatics Calculations based on Molecular Dynamics Free Energy Simulations . *J. Phys. Chem. B*. 101:5239–5248.

[12] Sigworth, F. J. 1993. Voltage gating of ion channels. *Quarterly Reviews of Biophysics*. 27:1–40.

Supplementary Table 3: List of the simulations performed[a]

Label	Length(ns)	Voltage(mV)	Start	Notes
SimOpen-eq	100	+500	KvOpen	equilibration
SimOpen-p	50	+500	SimOpen-eq	ΔQ, FEP
SimOpen-n	50	-500	SimOpen-eq	ΔQ, FEP
SimClosed-eq	100	-500	KvClosed	equilibration
SimClosed-p	50	+500	SimClosed-eq	ΔQ, FEP
SimClosed-n	50	-500	SimClosed-eq	ΔQ, FEP
SimVSD1-eq	50	+250	VSD1	equilibration
SimVSD1-p	50	+250	SimVSD1-eq	ΔQ
SimVSD1-o	50	0	SimVSD1-eq	ΔQ
SimVSD1-n	50	-250	SimVSD1-eq	ΔQ
SimVSD1-1V	10	+1000	SimVSD1-p	FEP
SimVSD1-0V	10	0	SimVSD1-p	FEP
SimVSD2-eq	100	-250	VSD2	equilibration
SimVSD2-p	50	+250	SimVSD2-eq	ΔQ
SimVSD2-o	50	0	SimVSD2-eq	ΔQ
SimVSD2-n	50	-250	SimVSD2-eq	ΔQ
SimVSD2-1V	10	-1000	SimVSD2-n	FEP
SimVSD2-0V	10	0	SimVSD2-n	FEP

[a] KvOpen and KvClosed refer to the full–length tetrameric models of the open and closed states of Kv1.2 (1), respectively. VSD1 and VSD2 refer to the individual, isolated voltage–sensor domains of KvOpen and KvClosed (residues 161–324), respectively.
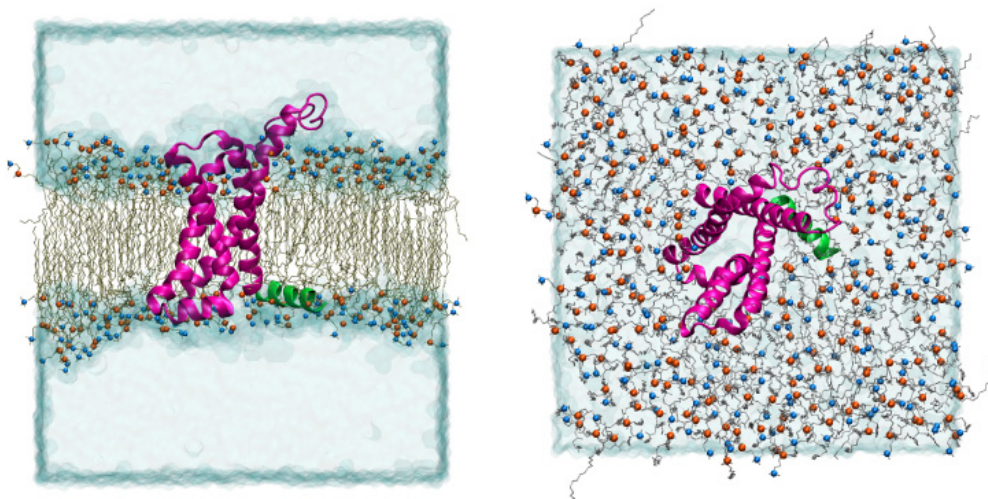
Supplementary Figure 1: Isolated voltage–sensor domain (VSD) of Kv1.2 in the active state in a patch of DPPC lipid bilayer. The snapshot is taken after the equilibration simulation. The protein backbone is shown in purple cartoon representation. The S4–S5 linker, connecting the VSD to the pore domain in the full–length channel, is highlighted in green. The atomic coordinates of the protein backbone on the S4-S5 linker were harmonically constrained during simulations of the VSD. Water molecules are shown in transparent blue surface representation. The lipid molecules are represented by lines with their oxygen and nitrogen atoms in vdW representation.
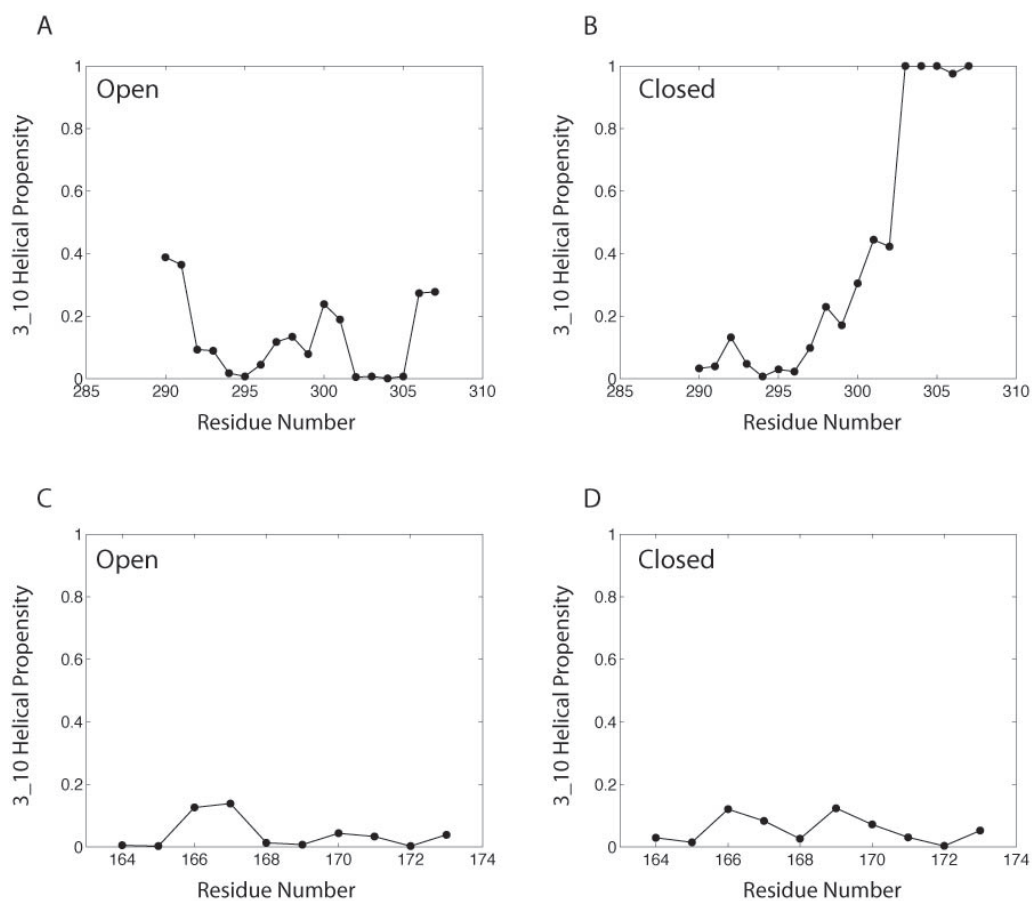
Supplementary Figure 2: The 3_{10}-helical propensity of S4 and S1 residues of an individual VSD is shown for the active (A,C) and resting (B,D) state conformations.

Supplementary Table 4: Salt bridge interactions within the VSD and between VSD and lipid molecules[a]

Residues	protein state	isolated VSD	(A)	(B)	(C)	(D)
R1-lipids	Active	0.94	0.39	0.97	0.97	0.95
R2-lipids	Active	0.81	0.66	0.38	0.14	0.49
R3-E0	Active	0.81	1.00	1.00	1.00	1.00
R3-E1	Active	0.42	1.00	0.79	0.97	1.00
R4-E1	Active	1.00	0.99	1.00	1.00	1.00
K5-D3	Active	0.99	0.99	1.00	0.98	0.89
K5-E2	Active	0.71	0.85	0.27	1.00	0.98
R6-E2	Active	0.00	0.16	0.99	0.00	0.00
R1-E0	Resting	0.34	0.91	0.42	0.91	0.93
R1-E1	Resting	0.00	0.02	0.99	0.09	0.41
R2-D3	Resting	0.00	0.38	0.00	0.25	0.93
R2-E2	Resting	0.00	0.10	0.60	0.23	0.25
R3-D3	Resting	0.00	0.01	0.94	0.00	0.00
R3-E2	Resting	0.00	0.99	0.00	0.79	0.00
R4-E2	Resting	0.00	0.00	0.99	0.00	0.00
K5-lipids	Resting	0.38	0.00	0.00	0.00	0.00
R6-lipids	Resting	0.41	0.85	0.71	0.81	0.81

[a] Salt-bridge probability for specific residues of the VSD calculated from the active and resting state trajectories SimOpen-p, and SimClosed-n of the full tetrameric channel, and SimVSD1-p and SimVSD2-n of the isolated VSD. Probability of salt-bridge formation between each residue pair is calculated as a fraction of the time where the distance between nitrogen and oxygen atoms of the two residues is smaller than 4 Å. The probabilities are presented for the isolated VSD and the four subunits (A–D) of the full-channel.

Supplementary Table 5: Fraction of transmembrane potential acting on each residue[a]

| Residue	Active(fullchannel)	Resting(fullchannel)	Active(VSD)	Resting(VSD)
R1	0.05 ± 0.06	-0.07 ± 0.07	-0.01	-0.21
R2	-0.07 ± 0.04	0.60 ± 0.06	0.18	0.78
R3	-0.01 ± 0.05	0.91 ± 0.04	0.04	1.05
R4	0.16 ± 0.04	0.89 ± 0.05	0.15	0.96
K5	0.89 ± 0.05	0.96 ± 0.04	0.52	0.93
R6	0.83 ± 0.05	0.96 ± 0.05	0.86	1.11
E1	0.16 ± 0.06	0.18 ± 0.06	0.17	0.02
E2	0.94 ± 0.05	0.86 ± 0.04	0.92	1.04
D3	1.02 ± 0.05	0.86 ± 0.07	0.86	0.96

[a]The fractional contributions were calculated from charging FEP/MD simulations one the active and resting states according to Eq. (3). The statistical uncertainty were estimated from the standard error of five independent FEP/MD runs for each residue.

Supplementary Table 6: Average Root Mean Square Deviation (RMSD) of the protein backbone of the VSD (residues 162-310) relative to the open or closed state conformations obtained after equilibration

Simulation	TM RMSD	TM RMSD (excluding S1-S2 loop)
SimOpen-p	2.7 Å	2.4 Å
SimOpen-n	2.6 Å	2.2 Å
SimClosed-p	6.7 Å	6.5 Å
SimClosed-n	3.9 Å	3.5 Å
SimVSD1-p	3.2 Å	2.2 Å
SimVSD1-o	3.9 Å	2.7 Å
SimVSD1-n	4.0 Å	2.8 Å
SimVSD2-p	2.6 Å	2.1 Å
SimVSD2-o	3.0 Å	2.7 Å
SimVSD2-n	2.8 Å	2.2 Å
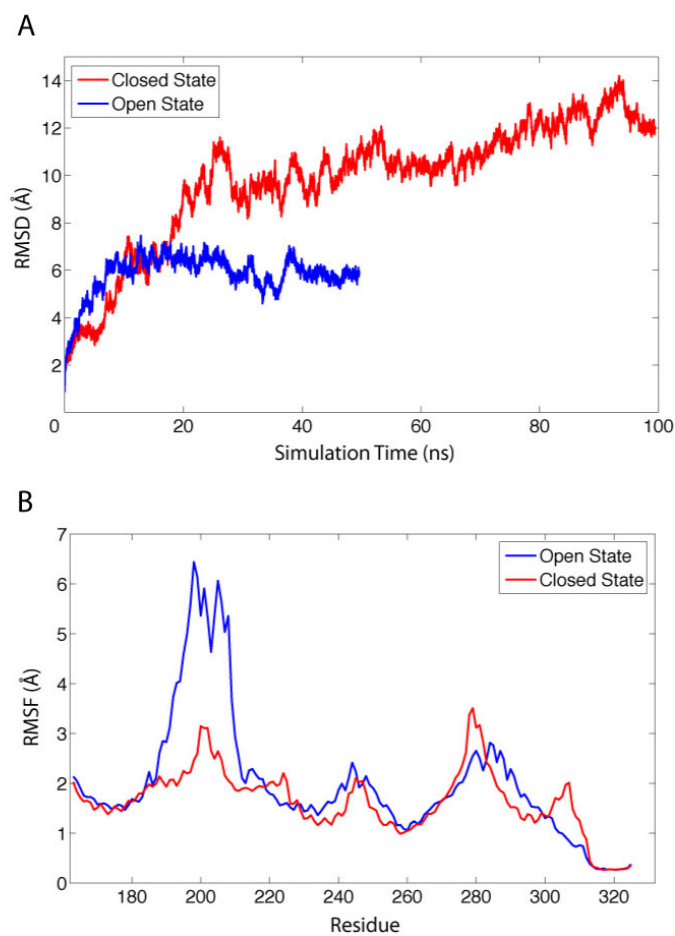
Supplementary Figure 3: (A) C_α root mean square deviation (RMSD) of the individual voltage-sensor domains (VSD) from the initial models (1) during the equilibration simulations (SimVSD1-eq and SimVSD2-eq). (B) C_α root mean square fluctuations (RMSF) of the VSD for each protein residue sampled from the 50 ns-simulations (SimVSD1-p and SimVSD2-n), that followed equilibration simulations.
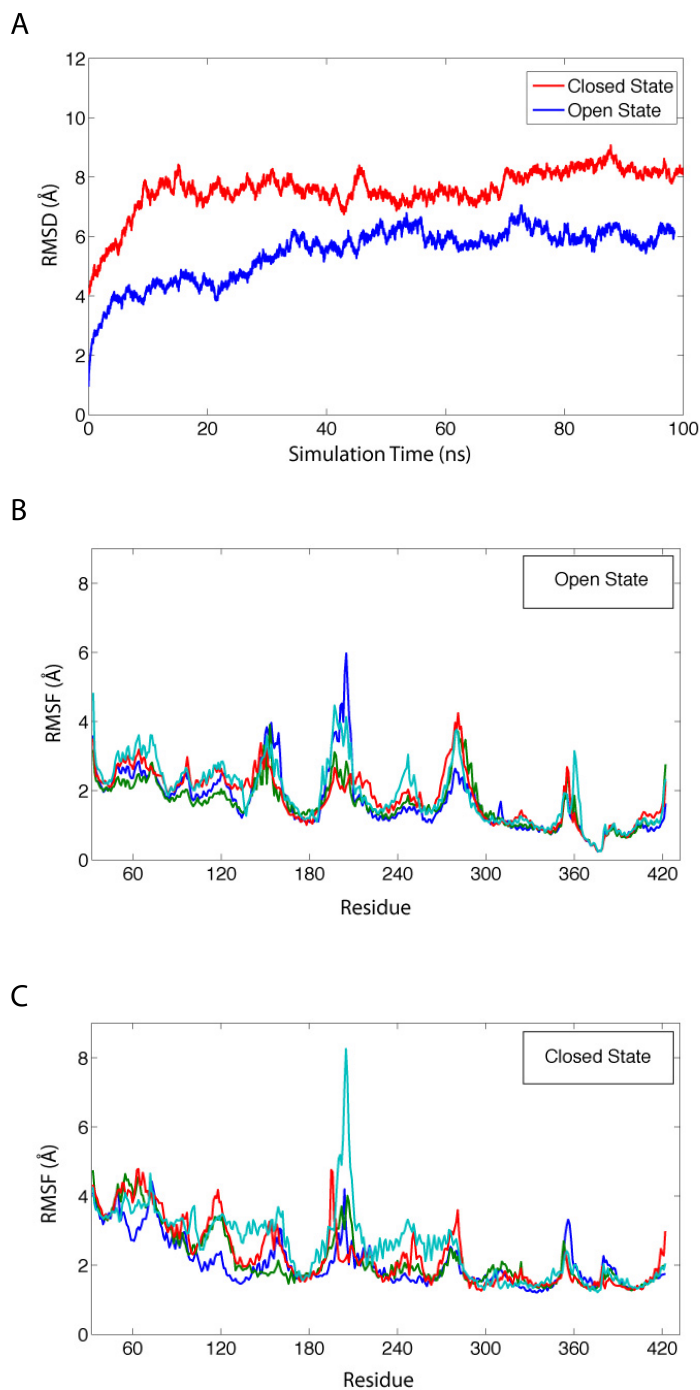
Supplementary Figure 4: (A) C_α root mean square deviation (RMSD) of the full tetrameric channel from the initial models (1) during the equilibration simulations. (B-C) C_α root mean square fluctuations (RMSF) of each protein residue during simulation SimOpen-p and SimClosed-n, of the open and closed state, respectively. The RMSF values the four protein subunits are colored differently.